Proceedings of the 33rd International Conference on Ocean, Offshore and Arctic Engineering
OMAE2014
June 8-13, 2014, San Francisco, USA

OMAE2014-23042

NUMERICAL INVESTIGATION OF WAVE-BODY INTERACTIONS IN SHALLOW WATER

Yi Luo
Dept. of Marine Technology, NTNU
Trondheim, Norway

Torgeir Vada
DNV
Høvik, Norway

Marilena Greco
Dept. of Marine Technology, NTNU,
AMOS, CNR-INSEAN
Trondheim, Norway

ABSTRACT

Present investigation is based on a numerical study using a time-domain Rankine panel method. The effort and novelty is to extend the applicability of the solver to shallower waters and to steeper waves by including additional non-linear effects, but in a way so to limit the increase in computational costs. The challenge is to assess the improvement with respect to the basic formulation and the recovery of linear theory in the limit of small waves.

The wave theories included in the program are Airy, Stokes 5th order and Stream function. By their comparison the effect of the incoming-wave non-linearities can be investigated.

For the free-surface boundary conditions two alternative formulations are investigated, one by Hui Sun [1] and one developed here.

The two formulations combined with the above-mentioned wave theories are applied to two relevant problems. The first case is a fixed vertical cylinder in regular waves, where numerical results are compared with the model tests by Grue & Huseby [2]. The second case is a freely floating model of a LNG carrier (with zero forward speed) in regular waves, where computations are compared with the experimental results from the EC project "Extreme Seas". This comparison revealed several challenges such as how to interpret/post process the experimental data. Some of these are described in the paper. After careful handling of both computed and measured data the comparisons show reasonable agreement. It is proven that including more non-linear effects in the free-surface boundary conditions can significantly improve the results. The formulation by Hui Sun gives better results compared to the linear condition, but the present formulation is shown to provide a further improvement, which can be explained through the nonlinear terms included/retained in the two approaches.

INTRODUCTION

The basic solver is a well established method for seakeeping problems in finite and deep water conditions with classical corrections for non-linear load terms. The restoring and Froude-Krylov pressures are computed at the instantaneous wetted body surface defined by the rigid body motions and the incident waves. The radiation/diffraction effects are estimated within linear theory, with the corresponding pressures integrated along the mean wetted surface, with the quadratic term in the Bernoulli equation included.

The performance of this method has been investigated in several papers, e.g. [3] and [4].

In order to extend the solver to shallow waters and steeper waves, two additional non-linear effects have been included and examined:

- A non-linear incoming-wave
- Some non-linear terms in the kinematic and dynamic free-surface boundary conditions

For the incoming wave, Stokes 5th order waves (using Fenton's formulation [5]) and Stream function (using Dalrymple's formulation [6]) have been included. In this study Stream function waves will be used since this has a wider applicability range than the Stokes waves.

In addition to the non-linearity of the incoming wave, other non-linear terms may be included in the free-surface elevation of the wave-body interaction problem. The issue in this context is consistency of the resulting solution method. A proposal in this direction is represented by the formulation in a previous work by Hui Sun [1]. An alternative strategy has been developed here as part of this work.

THE FREE-SURFACE BOUNDARY CONDITIONS

In a coordinate system moving with the steady velocity of the body, the exact free-surface boundary conditions may be written as

$$\frac{\partial(\phi_b+\phi_s+\phi_i)}{\partial z}=\left(\frac{\partial}{\partial t}-\vec{W}\cdot\nabla\right)(\zeta+\zeta_i)+\nabla(\phi_b+\phi_s+\phi_i)\cdot\nabla(\zeta+\zeta_i) \quad (1)$$

at $z=\zeta+\zeta_i$ (kinematic condition)

and

$$\left(\frac{\partial}{\partial t}-\vec{W}\cdot\nabla\right)(\phi_b+\phi_s+\phi_i)=-g(\zeta+\zeta_i)-\frac{1}{2}\left(\nabla(\phi_b+\phi_s+\phi_i)\right)^2 \quad (2)$$

at $z=\zeta+\zeta_i$ (dynamic condition)

Here $\vec{W}$ is the steady velocity of the vessel, ϕ_b is the steady velocity potential, ϕ_i and ζ_i are the velocity potential and wave elevation of the incoming wave, respectively, ϕ_s is the radiation and scatter velocity potential and ζ is the wave elevation due to the radiation/scatter and steady velocity potentials.

Since the steady speed may be large, the steady flow velocity potential can be assumed of order 1. Assuming all other quantities to be small and expanding the boundary conditions around the mean free surface, z=0, gives the linear boundary conditions used in the original solver.

The approach by Hui Sun.

In this formulation, all terms including the incoming wave are retained and evaluated at the instantaneous free surface. This gives the free-surface boundary conditions in the form

$$\left[\left(\frac{\partial}{\partial t}-\left(\vec{W}-\nabla\phi_b\right)\cdot\nabla\right)\zeta+\nabla\phi_b\cdot\nabla\zeta_i-\frac{\partial^2\phi_b}{\partial z^2}\cdot(\zeta+\zeta_i)-\frac{\partial\phi_s}{\partial z}\right]_{z=0}=\left[\frac{\partial\phi_i}{\partial z}-\left(\frac{\partial}{\partial t}-\vec{W}\cdot\nabla\right)\zeta_i-\nabla\phi_i\cdot\nabla\zeta_i\right]_{z=\zeta+\zeta_i} \quad (3)$$

$$\left[\left(\frac{\partial}{\partial t}-\left(\vec{W}-\nabla\phi_b\right)\cdot\nabla\right)\phi_s-\vec{W}\cdot\nabla\phi_b+g\zeta+\frac{1}{2}\left(\nabla(\phi_b)\right)^2+\nabla\phi_b\cdot\nabla\phi_i\right]_{z=0}=\left[-\left(\frac{\partial}{\partial t}-\vec{W}\cdot\nabla\right)\phi_i-g\zeta_i-\frac{1}{2}\left(\nabla(\phi_i)\right)^2\right]_{z=\zeta+\zeta_i} \quad (4)$$

If the right hand sides are set to 0, the linear free-surface conditions are recovered.

An attractive feature of this extension of the linear formulation is that the implementation is relatively straight forward since the new terms are computed directly from the incoming wave. A disadvantage of this formulation is that it is not consistent, because Taylor expansion about *z*=0 is only performed on the left hand side retaining terms of the order of the wave steeepness, say ε, and only ϕ_b is assumed *O*(1). The terms in the right hand side, which only include $\phi_i$and ζ_i without coupling with other variables, are retained and evaluated at the instantaneous free surface.

Present modified approach.

In this formulation we assume that $O(\phi_s)=O(\zeta)=O(\epsilon)$ and that $O(\phi_b)=O(\phi_i)=O(\zeta_i)=O(1)$. Expanding the exact equations and keeping the terms up to order ε gives

$$\left[\left(\frac{\partial}{\partial t}-\left(\vec{W}-\nabla\phi_b\right)\cdot\nabla\right)\zeta+\nabla\phi_b\cdot\nabla\zeta_i-\frac{\partial^2\phi_b}{\partial z^2}\cdot(\zeta+\zeta_i)-\frac{\partial\phi_s}{\partial z}\right]_{z=0}=\left[\frac{\partial^2\phi_i}{\partial z^2}\zeta-\frac{\partial(\nabla\phi_i\cdot\nabla\zeta_i)}{\partial z}\zeta-\nabla\phi_i\cdot\nabla\zeta-\nabla\phi_s\cdot\nabla\zeta_i\right]_{z=0} \quad (5)$$

$$\left[\left(\frac{\partial}{\partial t}-\left(\vec{W}-\nabla\phi_b\right)\cdot\nabla\right)\phi_s-\vec{W}\cdot\nabla\phi_b+g\zeta+\frac{1}{2}\left(\nabla(\phi_b)\right)^2+\nabla\phi_b\cdot\nabla\phi_i\right]_{z=0}=\left[-\zeta\left(\left(\frac{\partial}{\partial t}-\vec{W}\cdot\nabla\right)\frac{\partial\phi_i}{\partial z}+\nabla\phi_i\cdot\frac{\partial(\nabla\phi_i)}{\partial z}\right)-\frac{\partial(\nabla\phi_i\cdot\nabla\phi_b)}{\partial z}(\zeta+\zeta_i)-\nabla\phi_s\cdot\nabla\phi_i\right]_{z=0} \quad (6)$$

The left hand side of each condition is the same as in the Hui Sun's approach (and as in the linear conditions). Compared to that formulation, this one has a more consistent perturbation scheme since the whole equation is Taylor expanded and evaluated at *z*=0. This formulation also includes more non-linear terms in the form of coupling terms as both ϕ_i/ζ_i and ϕ_b are assumed *O(1)*, i.e. all coupling terms between ϕ_i/ζ_i and ϕ_s/ζ are retained and we no longer assume small incoming wave amplitude.

WAVE LOADS ON A FIXED CYLINDER

The first case we study is a fixed cylinder with a radius R of 3cm in 60cm water depth. This case was investigated experimentally by Huseby & Grue [2].

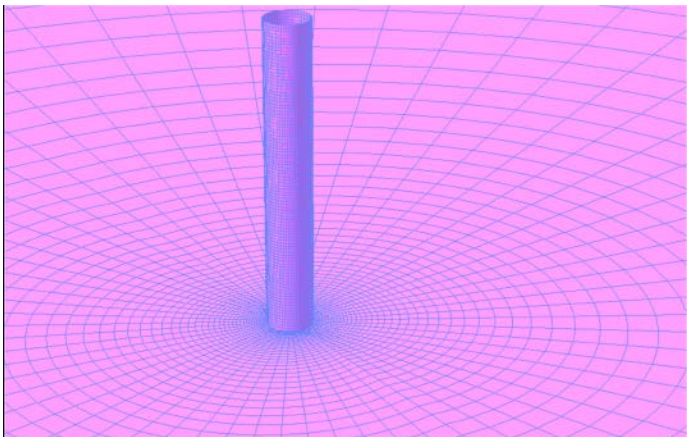

Figure 1. The mesh for the fixed cylinder case.

Computations of the horizontal force on the cylinder were performed for a wave with kR=0.245, with k the wavenumber, and with wave amplitude A of 0.03cm plus a sequence of amplitudes A ranging from 0.3cm to 3 cm with a step of 0.3 cm. The first 5 harmonic components of the force were extracted by using a least-square fit. Five different types of computations were performed:

- A linear analysis (green)
- A "classical" non-linear analysis with Airy wave (yellow)
- A "classical" non-linear analysis with Stream function wave (turquoise)
- Analysis with Stream function wave and the free-surface conditions by Hui Sun (red)
- Analysis with Stream function wave and the more consistent non-linear free-surface conditions (blue)

By "classical" non-linear analysis we mean an analysis including non-linear restoring and Froude-Krylov forces, but with linear free-surface conditions. In principle the list above contains the methods in increasing order of accuracy. The colors refer to the curves in figures 2-8.
The same problem has also been investigated by Ferrant [7] using a fully non-linear solution. His results are also included for comparison.
The water depth in this study is comparable with the wave length, meaning that we are basically studying infinite depth.
Figures 2 and 3 show the amplitude of the first and second harmonic component, respectively.

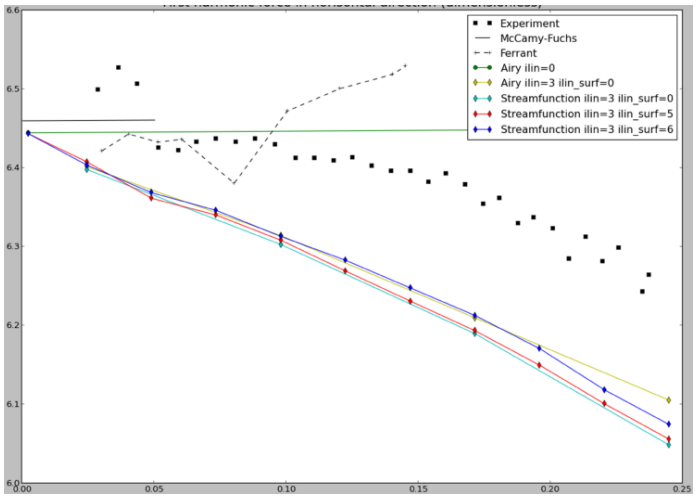

Figure 2. The first harmonic component of the dimensionless horizontal force, $|F_1|/(\rho g A R^2)$, as a function of kA.

From figure 2 we see that all the non-linear computations converge to the linear solution in the limit of very small waves. We also see that all the non-linear runs give very similar results. The trend is in good agreement with the experiments, but there seems to be a more or less constant difference. One may be tempted to assume that this difference is due to viscous forces, but this is not the case. The KC number in the experiments is in the range 1-3.6 and the Reynolds number is around 20000. Thus viscous forces can be assumed to be small.

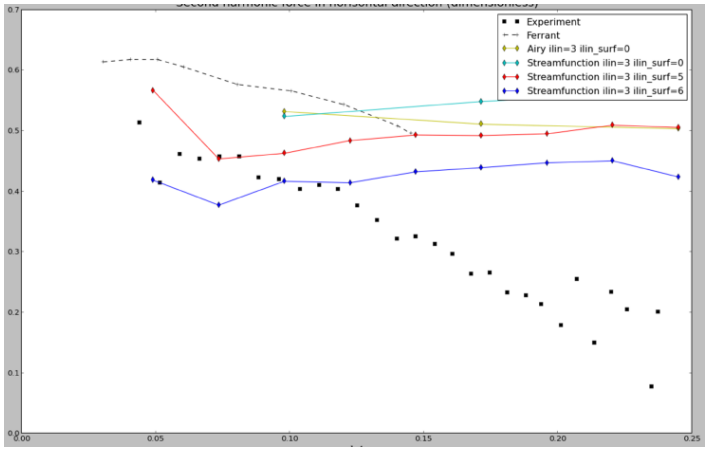

Figure 3. The amplitude of the second harmonic component of the dimensionless horizontal force, $|F_2|/(\rho g A^2 R)$, as a function of kA.

For the second harmonic component (see figure 3) there is as expected a more significant difference among the various methods and the most consistent (and also most non-linear) formulation shows the best agreement with the experiments. However, all formulations give a nearly constant value in kA which is not in accordance with the measured data. Here the solution by Ferrant provides a more correct trend even though the level is a bit high relative to the model tests.

In summary, the results by Ferrant overpredict both components, except at low values of kA, which probably indicates that the total force is overpredicted. For the methods investigated in this paper the overall conclusion is that they seem to under predict the first harmonic component and to over predict the second one. This indicates that the computations have a more asymmetric behavior around the mean value than the experiments. In addition, we notice that both methods have one component with the correct trend, but the trend is wrong for the other component. This may indicate that there is some uncertainty in the split between the two components.

The phase angles for the first and second harmonic components of the horizontal force on the cylinder are shown in figures 4 and 5.

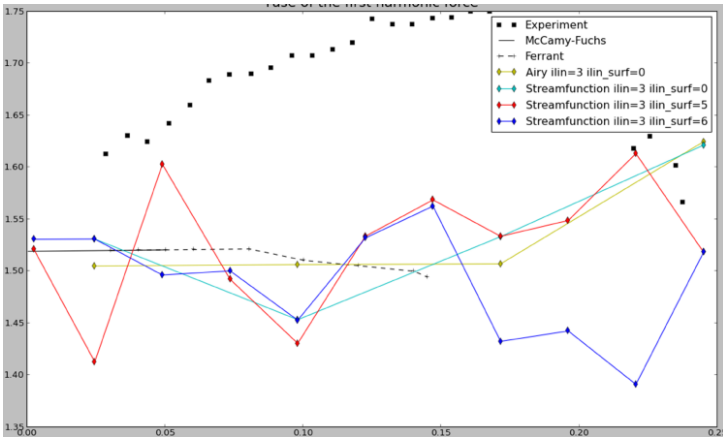

Figure 4. The phase angle of the first harmonic component of the horizontal force, Arg(F_1), as a function of kA.

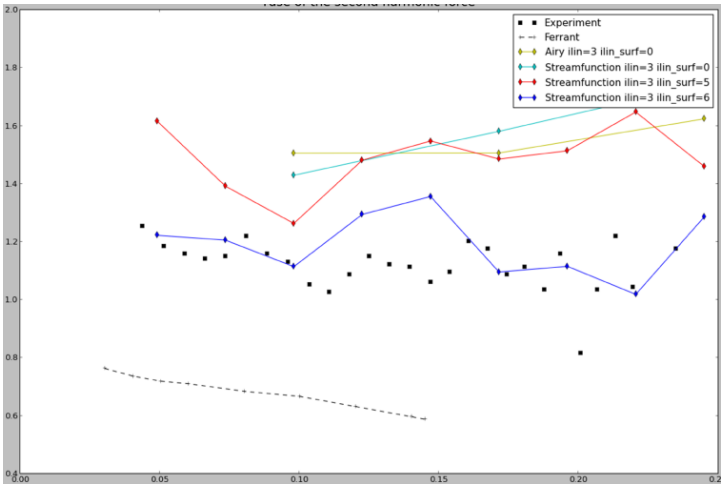

Figure 5. The phase angle of the second harmonic component of the horizontal force, Arg(F_2), as a function of kA.

When we try to fit an asymmetric signal with a symmetric function by the method of least squares, the solution will not be unique due to more than one possible convergence direction (you may consider the non-square linear algebra problem **A**x = b in a geometrical interpretation as to find the orthogonal projection of b on the range of **A** iteratively). An asymmetry in one direction may cause two symmetric functions with different amplitudes and phases but with the same least-square error. The oscillatory nature of the phase angle as shown in figure 4 may be an indication that we have such a problem here.

A more robust comparison is thus to compare directly the measured horizontal force time history against the numerical evolution from the different formulations. This quantity is free from identification errors, because it is the variable recorded experimentally. Since both amplitudes and phase angles of the first 6 harmonics in the experiments are given in Huseby & Grue it is easy to reconstruct the force time history.

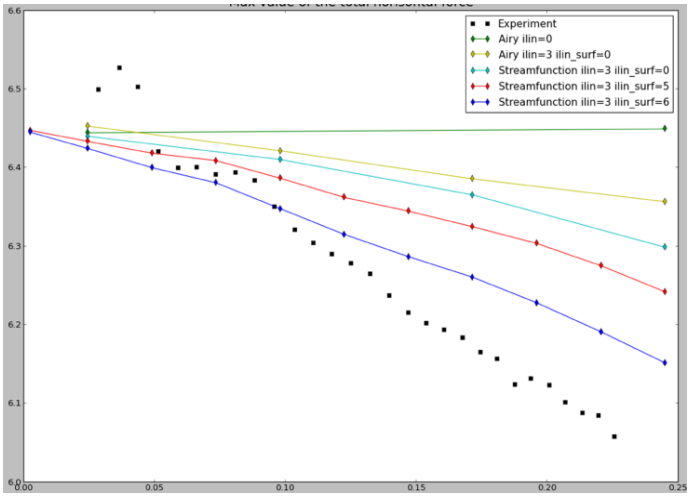

Figure 6. The maximum value of the dimensionless horizontal force, $F_{max}/(\rho g A R^2)$, as a function of kA.

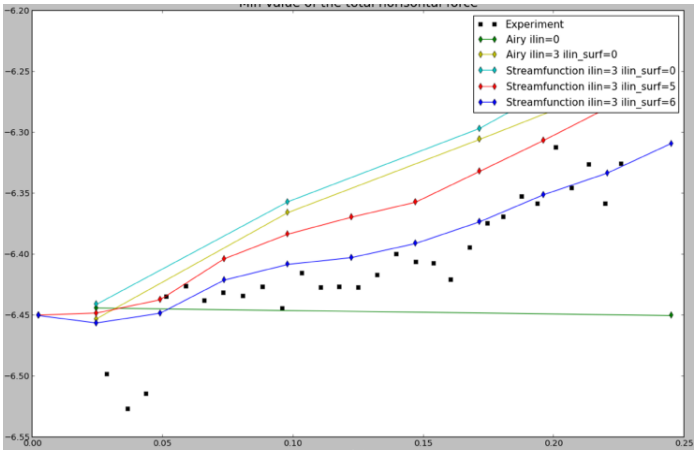

Figure 7. The minimum value of the dimensionless horizontal force, $F_{min}/(\rho g A R^2)$, as a function of kA.

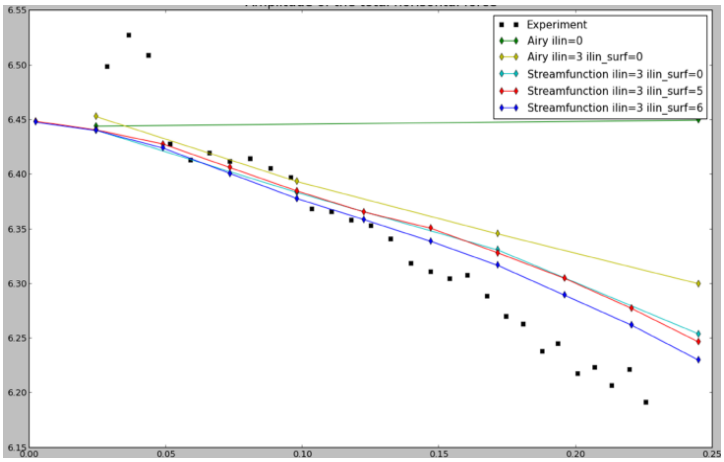

Figure 8. The amplitude of the dimensionless horizontal force, $0.5(F_{max}-F_{min})/(\rho g A R^2)$, as a function of kA.

Figure 6 and 7 show the comparison of the minimum and maximum force. It confirms that the most consistent method gives the best agreement with the experiments. For this formulation the total-force comparisons are good both in terms of trends and quantitatively; this supports the idea that the disagreement for the first and second harmonic components could be partially due to problems in their identification procedure. The more simplified formulations over predict the maximum value of the force and under predict the minimum value. We also notice that the non-linear free-surface conditions have more influence on the results than the nonlinearity in the incoming wave. If we, however, examine the horizontal force amplitude (defined as half the difference between maximum and minimum values) the picture is somewhat different. Here the wave formulation has the most important influence on the results. This is shown in figure 8.

SHIP MOTIONS IN STEEP REGULAR WAVES

The next case to be studied is the wave induced motion of a LNG carrier, see figure 9. The investigation covers different wave steepnesses and different wave lengths. For the longest waves the effect of finite depth can be expected to be significant. The computations are done in full scale. The model tests are done as part of the EC project “Extreme waves”. The data for the vessel are given in table 1.

Twenty-two different waves were analyzed. The wave parameters are listed in table 2. The waves fall into two groups: Waves 1-11 are waves of moderate amplitude. We will refer to them as series 1. These waves are just outside the validity range of the Airy wave theory. Waves 12-22 have much higher wave amplitudes and some of them are outside the validity range of the Stokes 5^{th} order theory. This is illustrated in figure 10. We will refer to these waves as series 2.

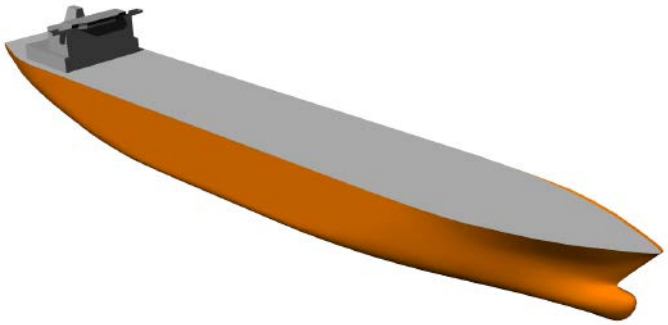

Figure 9. The LNG vessel.

Scale = 70	Full scale	Model
Loa	197.13 m	2.816 m
Lpp	186.90 m	2.670 m
B	30.38 m	0.434 m
D	18.20 m	0.268 m
d	8.40 m	0.120 m
M	35614.03 t	103.831 kg
CGx	94.87 m	1.355 m
CGy	0.00 m	0.000 m
CGz	8.26 m	0.118 m
RGx	11.27 m	0.161 m
RGy	40.53 m	0.579 m
RGz	40.18 m	0.574 m
Water Depth	70 m	1 m

Table 1. The dimensions of the LNG carrier.

The interpretation of the measured ship-motion time histories poses some challenges as illustrated in figures 11 and 12. In particular the heave response has a rather unsteady behavior, whereas the pitch response seems to have better quality. It is also unclear why there is a significant mean displacement in heave.

In the comparison between the computations and measurements we show the response amplitude. This is defined as half the difference between the maximum and minimum of the response. Thus the mean displacement in heave is not a part of this comparison. We have also computed the mean value and standard deviation of the amplitudes. The standard deviation is shown as the error band in the results in figures 13-16.
Fifteen waves are applied in the results presented by figures 13-16, where the numbers indicate the incoming-wave number in Table 2.The computations are done both with the fully linear solver (blue curve) and with the most non-linear solver which includes stream function wave and the consistent non-linear free-surface conditions (red curve). As expected the two solutions are almost identical for wave series 1. The pitch response is in perfect agreement with the measurements. For

heave there is a small deviation for waves 6 and 8, but the rest of the results are very good.

Wave	λ	H	T	H/gT^2	d/gT^2	kA
1	112.14	2	8.4664	0.00284	0.09955	0.05603
2	149.52	2	9.8062	0.00212	0.07420	0.04202
3	168.21	3	10.4204	0.00282	0.06571	0.05603
4	186.90	3	11.0277	0.00251	0.05868	0.05043
5	205.59	3	11.6243	0.00226	0.05281	0.04584
6	224.28	4	12.2062	0.00274	0.04789	0.05603
7	261.66	4	13.3867	0.00228	0.03982	0.04803
8	299.04	5	14.5667	0.00240	0.03363	0.05253
9	336.42	5	15.7731	0.00205	0.02868	0.04669
10	373.80	6	16.9870	0.00212	0.02473	0.05043
11	411.18	6	18.2304	0.00184	0.02147	0.04584
12	112.14	8	8.2690	0.01193	0.10436	0.22412
13	149.52	11	9.5532	0.01229	0.07819	0.23112
14	168.21	12	10.1723	0.01182	0.06896	0.22412
15	186.90	13	10.7714	0.01142	0.06150	0.21852
16	205.59	14	11.3575	0.01106	0.05532	0.21393
17	224.28	16	11.8956	0.01153	0.05043	0.22412
18	261.66	18	13.0404	0.01079	0.04196	0.21612
19	299.04	20	14.1784	0.01014	0.03550	0.21011
20	336.42	22	15.3139	0.00956	0.03043	0.20544
21	373.80	24	16.4456	0.00905	0.02638	0.20171
22	411.18	25	17.6203	0.00821	0.02298	0.19101

Table 2. The waves included in the analysis (full scale).

For several waves in wave series 2 there is a significant difference between the linear and the non-linear result. For pitch the non-linear solution is clearly better. For heave the linear results actually seems to be better, but it should be kept in mind that there is a significant uncertainty in the measurements for heave.

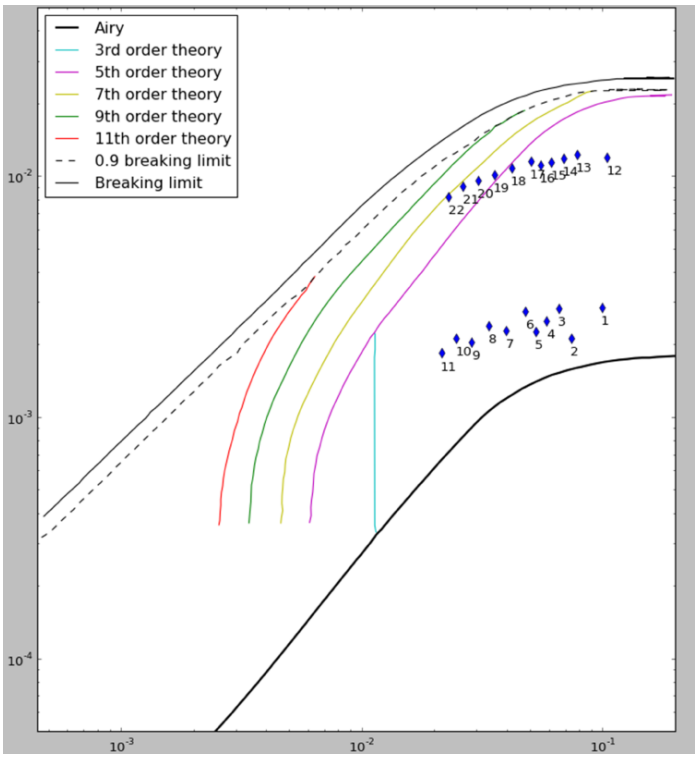

Figure 10. The waves to be studied plotted in the theory validity range diagram. In the horizontal axis: d/gT^2; in the vertical axis: H/gT^2.

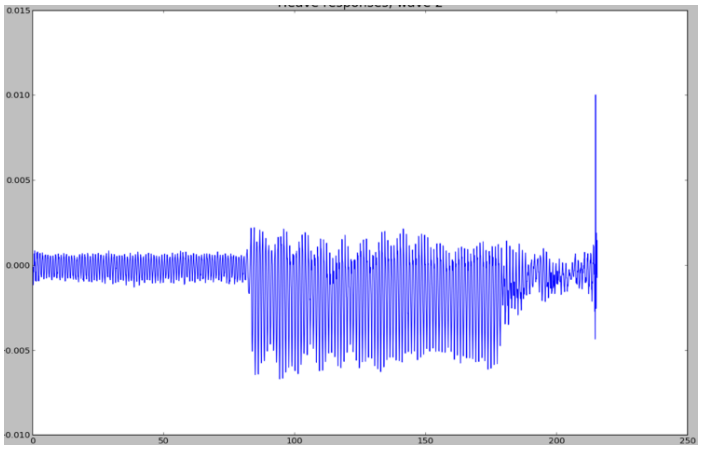

Figure 11. Measured time history (in seconds) of the heave motion (in meters) for wave 2.

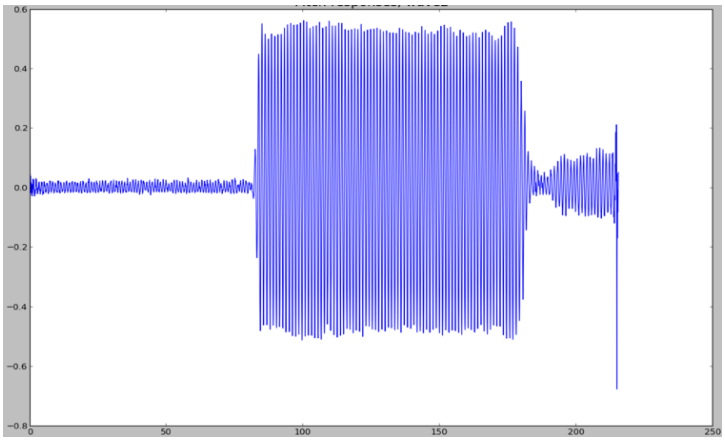

Figure 12. Measured time history (in seconds) of the pitch motion for wave 2.

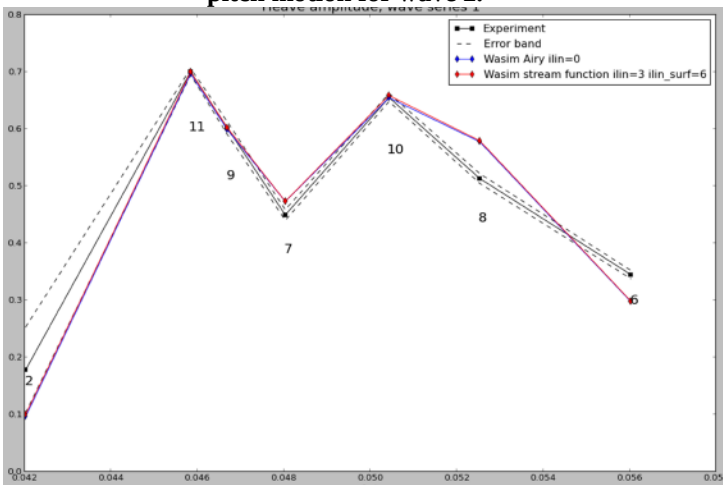

Figure 13. The heave RAO, $|\eta_{3,max}-\eta_{3,min}|/(2\zeta_a)$ (with ζa=A), for wave series 1 as a function of kA.

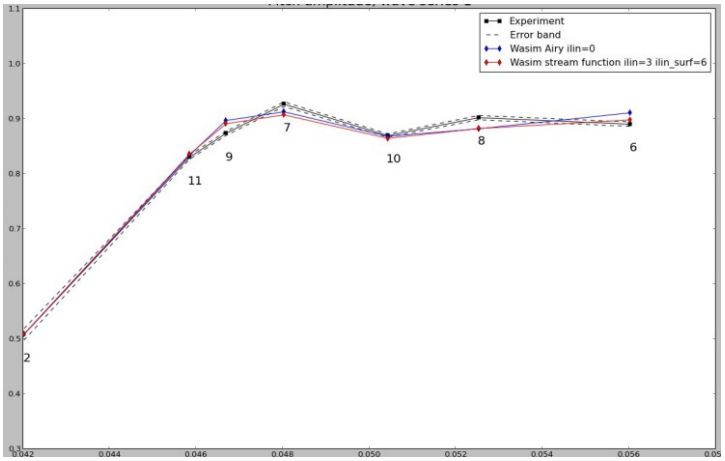

Figure 14. The pitch RAO, $|\eta_{5,max}-\eta_{5,min}|/(2\zeta_a)$ (with ζa=A), for wave series 1 as a function of kA.

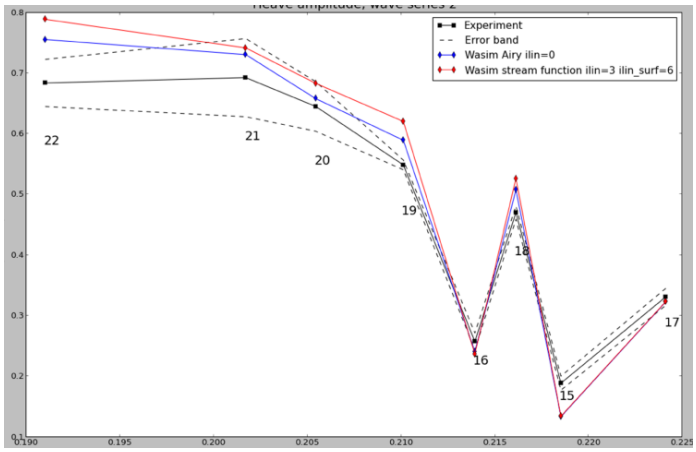

Figure 15. The heave RAO, $|\eta_{3,max}-\eta_{3,min}|/(2\zeta_a)$ (with ζa=A), for wave series 2 as a function of kA.

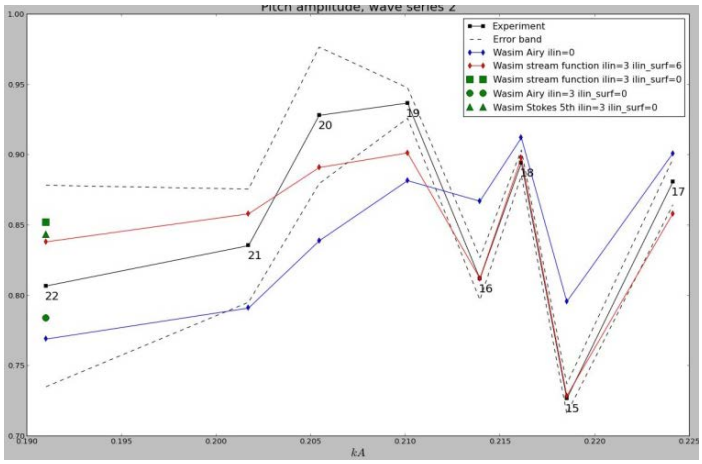

Figure 16. The pitch RAO, $|\eta_{5,max}-\eta_{5,min}|/(2\zeta_a)$ (with ζa=A), for wave series 2 as a function of kA.

For the most extreme wave, wave 22, additional runs have been done with different wave theories, but linear free-surface conditions. These results are shown by the green markers in figure 16 (pitch). The result for the Airy wave is almost the same as from the linear solution, whereas the results for the Stokes 5th order wave and Stream function wave are almost the same as for the most non-linear solution. Thus it is clear that the dominating non-linear effect is the non-linearity in the incoming wave. One should note that this wave corresponds to a quite shallow water condition, since the wave length is almost 6 times the water depth (411.2m vs. 70m).

For this wavelength a final set of computations were performed for different wave amplitudes. The purpose of this is to check that the most non-linear analysis converges to the linear results in the limit of small waves. This fact is confirmed by results in figures 17 and 18.

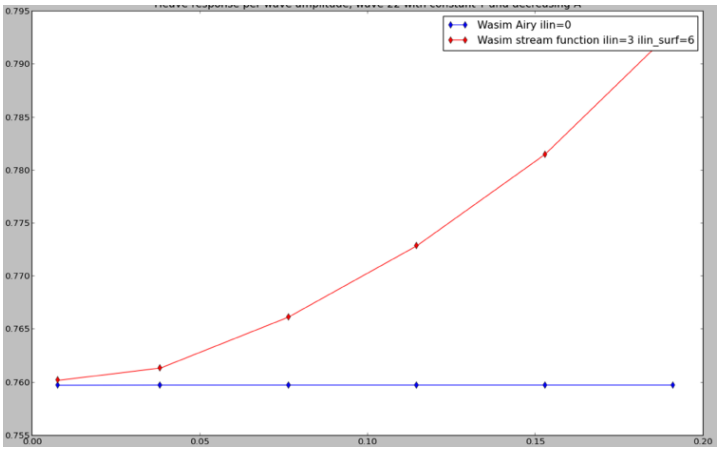

Figure 17. Comparison of heave RAOs, $|\eta_{3,max}-\eta_{3,min}|/(2\zeta_a)$ (with $\zeta a=A$), from the linear and non-linear solution for the largest wave length examined with varying wave amplitude as a function of kA.

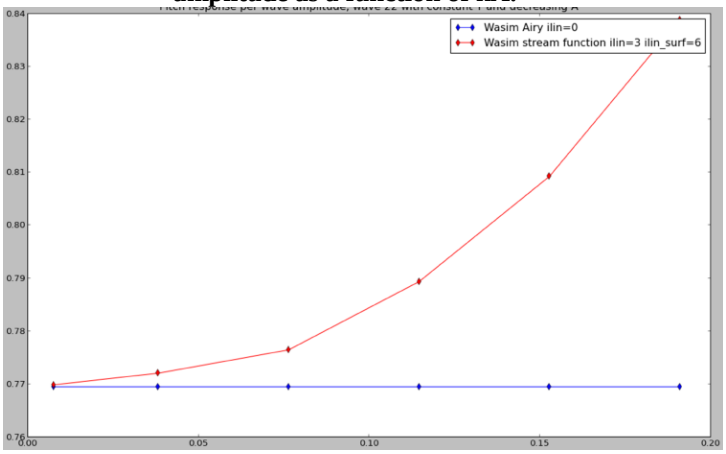

Figure 18. Comparison of pitch RAOs, $|\eta_{5,max}-\eta_{5,min}|/(2\zeta_a)$ (with $\zeta a=A$), from the linear and non-linear solution for the largest wave length with varying wave amplitude as a function of kA.

CONCLUSIONS

A numerical investigation has been carried out based on a time-domain Rankine panel method for wave-body interaction problems. The purpose of this study is to investigate the importance of non-linear wave theories and the importance of non-linear terms in the free-surface boundary conditions for steep waves. In addition to a previous implementation of some non-linear terms in the free-surface conditions, a new and more consistent formulation based on the assumption that the incoming wave is not small has been proposed. The main motivation for the development is to extend the applicability of the solver to shallower water conditions, but the non-linear free-surface conditions may be equally important for large waves in deep water.

The latter statement is confirmed by the comparison for a fixed vertical cylinder. The water depth in this investigation (60 cm) is only slightly less than the wave length (77 cm) so this is a deep water case. In this case it is shown that the non-linear free-surface conditions can give a significant improvement of the results, with the new and more consistent formulation as the best choice. The non-linearity in the incoming wave seems to be less important.

The other case studied is a floating body in relatively shallow water. Here the non-linearity in the incoming-wave provides the dominant corrections of the results while the non-linear terms in the free-surface conditions seem to be of minor importance. But in this case, the waves are relatively long to the ship so we need to take into account that both wave diffractions and radiations are small.

So from present studies, in general non-linearities in the incident waves and in the free-surface boundary conditions are both important in steep waves. It is hard to make a strong conclusion about which one is more important than the other because this depends on several factors. If we only consider the water depth, then the free-surface boundary conditions plays the major role in deep water while the non-linearities in the incident waves become more important in shallower water.

Present method extended the applicability of a basically linear solver to higher incident-wave steepness. However a kA limit exists in terms of results reliability. On the other hand we cannot identify this limit just on the basis of two validation studies, though relevant for our case. As a future step, a more comprehensive research investigation should be carried out for a complete assessment of the applicability limits. Identifying the responsible of these limitations could inspire a further improvement of the proposed formulation.

ACKNOWLEDGMENTS

This work builds on previous work funded by the EC project “Extreme seas”. Also the experimental results from this project were made available. This support is highly appreciated. One of the co-authors is connected with the Centre of Excellence AMOS, supported by the Research Council of Norway through the Centres of Excellence funding scheme AMOS, project number 223254.

REFERENCES

[1] **Sun, Hui**, *A method based on Wasim to simulate ship responses in large amplitude incident waves*, Extreme seas, D-4.1-DNV, June 2012 (confidential).

[2] **Huseby, M. & Grue, J.,** *An experimental investigation of higher-harmonic wave forces on a vertical cylinder*, Journal of Fluid Mechanics, Vol. 414, pp. 75–103, 2000.

[3] **Pastoor, W., van't Veer, R. & Harmsen, E.,** *Seakeeping behavior of a frigate type trimaran*, RINA RINA International Conference on the Design and Operation of Trimaran Ships, London, UK, 2004.

[4] **Pastoor, W. & Tveitnes, T.,** *Rational Determination of Nonlinear Design Loads for Advanced vessels*, FAST 2003, Naples, Italy, 2003, pp. 41-48.

[5] **Fenton, J. D.**, *A fifth-order Stokes theory for steady waves*, Journal of Waterway, Port, Coastal and Ocean engineering, Vol. 111, No. 2, pp. 216-234, March 1985.

[6] **Dalrymple, A.R**., *A finite amplitude wave on a linear shear current*. Journal of Geophysical Research, Vol. 79, Issue 30, pp. 4498-4504, October 1974.

[7] **Ferrant, Pierre**, *Fully non-linear interactions of long crested wave packets with a three-dimensional body*, 22nd ONR Symposium on Naval Hydrodynamics, Washington DC, August,1998, pp. 403-415.